Received: 20 September 2021 | Revised: 9 November 2021 | Accepted: 16 November 2021

DOI: 10.1002/psp4.12750

ARTICLE

Physiologically-based pharmacokinetic modeling of oxcarbazepine and levetiracetam during adjunctive antiepileptic therapy in children and adolescents

Jaydeep Sinha[1,2] | **Eleni Karatza**[1] | **Daniel Gonzalez**[1]

[1]Division of Pharmacotherapy and Experimental Therapeutics, UNC Eshelman School of Pharmacy, The University of North Carolina at Chapel Hill, Chapel Hill, North Carolina, USA

[2]Department of Pediatrics, UNC School of Medicine, The University of North Carolina at Chapel Hill, Chapel Hill, North Carolina, USA

Correspondence
Daniel Gonzalez, Division of Pharmacotherapy and Experimental Therapeutics, UNC Eshelman School of Pharmacy, The University of North Carolina at Chapel Hill, 301 Pharmacy Lane, Campus Box #7569, Chapel Hill, NC 27599-7569, USA.
Email: daniel.gonzalez@unc.edu

Funding information
This research was funded by the Eunice Kennedy Shriver National Institute of Child Health and Human Development (NICHD) under awards 5R01HD096435-03 and 1R01HD102949-01A1 (PI: Gonzalez). E.K. was funded through the University of North Carolina at Chapel Hill/GlaxoSmithKline Pharmacokinetics/Pharmacodynamics Fellowship. The content is solely the authors' responsibility and does not necessarily represent the official views of the National Institutes of Health.

Abstract

Oxcarbazepine (OXZ) and levetiracetam (LEV) are two new generation antiepileptic drugs, often co-administered in children with enzyme-inducing antiepileptic drugs (EIAEDs). The anti-epileptic effect of OXZ and LEV are linked to the exposure of OXZ's active metabolite 10-monohydroxy derivative (MHD) and (the parent) LEV, respectively. However, little is known about the confounding effect of age and EIAEDs on the pharmacokinetics (PKs) of MHD and LEV. To address this knowledge gap, physiologically-based pharmacokinetic (PBPK) modeling was performed in the PK-Sim software using literature data from children greater than or equal to 2 years of age. Age-related changes in clearance (CL) of MHD and LEV were characterized, both in the presence (group 1) and absence (group 2) of concomitant EIAEDs. The drug-drug interaction effect of EIAEDs was estimated as the difference in CL estimates between groups 1 and 2. PBPK modeling suggests that bodyweight normalized CL (ml/min/kg) is higher in younger children than their older counterparts (i.e., due to an influence of age). Concomitant EIAEDs further increase MHD's CL to a fixed extent of 25% at any age, but EIAEDs' effect on LEV's CL increases with age from 20% (at 2 years) to 30% (at adolescence). Simulations with the maximum recommended doses (MRDs) revealed that children between 2 and 4 years and greater than 4 years, who are not on EIAEDs, are at risk of exceeding the reference exposure range for OXZ and LEV, respectively. This analysis demonstrates the use of PBPK modeling in understanding the confounding effect of age and comedications on PKs in children and adolescents.

Study Highlights

WHAT IS THE CURRENT KNOWLEDGE ON THE TOPIC?

Concomitant use of enzyme-inducing anti-epileptic drugs (EIAEDs) is common in children receiving oxcarbazepine (OXZ) or levetiracetam (LEV), which potentially confounds the age-related variability in the pharmacokinetics (PKs) of OXZ's active metabolite 10-monohydroxy derivative (MHD) and LEV.

WHAT QUESTION DID THIS STUDY ADDRESS?

This analysis systematically assessed the drug-drug interaction (DDI) potential of EIAEDs by delineating it from the influence of age on PKs in children greater than or equal to 2 years of age.

WHAT DOES THIS STUDY ADD TO OUR KNOWLEDGE?

Younger children have higher bodyweight normalized clearance (CL) than their older counterparts. Additionally, concomitant EIAEDs increase the CL of MHD to a fixed extent of 25% (i.e., a fixed DDI effect). However, the DDI effect on LEV's CL increases with age from 20% (at 2 years) to 30% (at adolescence), implying an age-dependent DDI.

HOW MIGHT THIS CHANGE DRUG DISCOVERY, DEVELOPMENT, AND/OR THERAPEUTICS?

This analysis reiterates that the DDI effect in children can vary with age for certain drugs (e.g., LEV), warranting more precise dosing. Physiologically-based pharmacokinetic modeling is a useful approach for the assessment of age-dependent DDI.

INTRODUCTION

Understanding the variation in drug clearance (CL) is essential for determining dosing recommendations in the pediatric population, where a change in CL is anticipated compared to the adult population. Age-related changes in CL are linked to the structural (e.g., organ size) and functional (e.g., metabolic activity) changes in physiology throughout childhood due to the growth and maturation in the drug-eliminating organs. However, understanding the age-related variation in CL is not always straightforward in children.

In children, clinical pharmacology studies are exclusively performed in patients, rarely involving healthy volunteers (unlike adults). Understanding the age-related changes in CL may become challenging while leveraging data from a patient population due to potential confounding effects of disease- and treatment-related factors, such as organ dysfunction and comedications, respectively. Oxcarbazepine (OXZ) and levetiracetam (LEV) are two new-generation anti-epileptic drugs (AEDs), where the effect of age on CL is potentially confounded by the concomitant use of enzyme-inducing AEDs (EIAEDs), such as phenobarbital, phenytoin, or carbamazepine, during adjunctive antiepileptic therapy. Adjunctive therapy (i.e., co-administration) with OXZ or LEV is indicated in children greater than 2 years and greater than 1 month of age, respectively, when a conventional first-line AED (that often includes an EIAED) fails to control seizure recurrence.[1–3]

OXZ is available as tablet and suspension formulations. Following oral administration, OXZ is completely absorbed[4] and rapidly converted to its active metabolite 10-monohydroxy derivative (MHD) by a set of cytosolic enzymes known as aldo-keto reductases (AKRs), ubiquitously expressed in various tissues.[5–7] The formation of MHD is rapid and complete, as evidenced by its high formation CL (175 L/h) and nearly 100% absolute bioavailability following an oral OXZ dose.[8] On the other hand, the elimination CL of MHD is slow (~3.5 L/h) and mediated mainly by glucuronide conjugation and renal excretion, accounting for about half and one-fourth of the dose, respectively.[8] A rapid formation and a subsequent slow elimination result in an ~45-fold higher exposure of MHD than OXZ following oral administration of OXZ. Therefore, the anti-epileptic effect of OXZ has been linked to the exposure of MHD.[8] LEV is administered both orally (as a tablet and solution) and intravenously (i.v.). After oral administration, it is completely absorbed, mainly eliminated by renal excretion (nearly 70% of dose) with substantial tubular reabsorption, resulting in a low CL (~4 L/h). The remainder of the LEV dose is mainly metabolized by a specific set of esterase enzymes (known as Type B esterases) that are expressed within red blood cells (RBCs).[9-11] The pharmacokinetics (PKs) of OXZ and LEV are known to be dose-proportional up to 2700 mg and 4000 mg, respectively, and these doses are beyond the typical clinical dose range in adults.[7,12–14]

The current dosing recommendations of OXZ and LEV suggest varying bodyweight normalized doses (mg/kg) for different age groups of children.[1,2] Such a dosing scheme accounts for the influence of age on CL in pediatric patients. For example, a two-fold higher OXZ dose is recommended for children between 2 and 4 years than those above 4 years of age to account for the higher CL (ml/min/kg) in the younger age group than in their older counterpart.[1]

However, information about the potential influence of EIAEDs (during adjunctive therapy) on dosing is limited. The concomitant EIAEDs can enhance the CL of OXZ and LEV because both drugs undergo substantial metabolism. Therefore, it is essential to understand whether such influence of EIAEDs exists to a clinically relevant extent and to what extent it influences the age-related changes in CL. A systematic analysis is needed to address this question, which would help inform dosing in children.

Physiologically-based pharmacokinetic (PBPK) modeling can be used to address this question because the influence of age and EIAEDs on PKs can be separated on a mechanistic basis. PBPK modeling has the unique ability of bottom-up scaling of PKs from the drug-specific properties generated in vitro/in silico, thereby obviating the need for extensive PK data in the target population. This is particularly useful for understanding the change in CL in pediatric patients where data are limited. Therefore, the aim was to characterize the effect of age on CL of MHD and LEV in children and adolescents (i.e., baseline change in CL) through PBPK modeling and thereby estimate any potential impact of EIAEDs after delineating the effect of age on PKs.

METHODS

Data

Three types of literature data were collected: (1) estimates of the drug-specific properties that include the physicochemical properties, such as solubility and lipophilicity (LogP); (2) drug disposition properties such as intrinsic CL (CL_{int}), free fraction in plasma ($f_{u,p}$); and (3) data of plasma concentration-time (C-T) and urinary excretion-time (E-T) profiles following i.v. and oral administrations, which were extracted using the PinPoint software (version 0.2.0). The details of the studies, including the patient characteristics, are summarized in Tables S1 and S2 of the Electronic Supplementary Material (ESM).

Model development

Modeling was performed using the whole-body PBPK framework implemented in the PK-Sim software (version 9.1; Open Systems Pharmacology Suite, open-systems-pharmacology.org). Briefly, separate PBPK models were developed for OXZ and LEV in adults. The OXZ model included two inter-linked submodels for OXZ and MHD, where MHD is formed following oral administration of OXZ post-absorption. First, the initial estimates of the drug-specific properties were leveraged from the literature. Then, key parameter estimates (e.g., CL_{int}) were optimized using average C-T and E-T data from three reported clinical studies in adults[8,11,13] that included i.v. and oral data of MHD, OXZ, and LEV. PK-Sim's built-in Monte-Carlo optimization algorithm was initially used. For some parameters, the optimization outputs were slightly manually adjusted to improve the visual data fit further. Additional descriptions of the model considerations are provided in section S1.2 of the ESM.

Oxcarbazepine model

First, the literature derived estimates of $f_{u,p}$, LogP, hepatic CL_{int} ($CL_{int,H}$), and renal CL_{int} ($CL_{int,R}$) of MHD were inputted, which did not produce a reasonable fit to the observed mean C-T and E-T data following i.v. administration of MHD in healthy adults.[8] Finally, LogP, $CL_{int,H}$, and $CL_{int,R}$ estimates were optimized to fit the data.

In the next step, the processes related to OXZ's (1) dissolution in the gastrointestinal (GI) lumen, (2) its conversion to MHD within the enterocytes (during permeation) and other tissues (post-permeation), (3) the GI permeation of both OXZ and MHD into basolateral circulation, and (4) OXZ's distribution (Figure S1) were modeled simultaneously to predict the OXZ and MHD plasma C-T data following oral administration of OXZ. To describe the dissolution (process 1), an empirical Weibull dissolution model with zero lag time was considered, where the initial estimates of solubility, dissolution shape, and the time to dissolve 50% of tablet strength ($T_{50\%}$) were 0.30 mg/ml,[15] 0.8,[16] and 30 min, respectively.[16] To describe the formation of MHD (process 2), OXZ's intrinsic clearance data ($CL_{int,AKR}$) from incubations of four recombinant AKR isoforms (AKR1C1, AKR1C2, AKR1C3, and AKR1C4) were used.[17] Because these isoforms' abundance were unknown, PK-Sim's default value of 1 μmol/L was assumed for each of them. Their relative tissue distribution data were extracted from the Open Systems Pharmacology gene expression database. Importantly, for the formation of MHD (process 2), the key assumption was that OXZ is exclusively eliminated via reduction to MHD because greater than 95% of the OXZ dose is recoverable in urine as either unchanged MHD or its glucuronide conjugate. Permeation (of OXZ and MHD) and distribution of OXZ (processes 3 and 4) were accounted for by inputting LogP, the transcellular intestinal permeabilities of OXZ and MHD ($P_{eff,trans}$, that were generated by PK-Sim from LogP input), and the $f_{u,p}$ of OXZ. The final model of OXZ was developed by optimizing the estimates of $T_{50\%}$, $CL_{int,AKR}$ (for all 4 isoforms), and $P_{eff,trans}$ of OXZ to simultaneously fit the mean plasma C-T data of OXZ and MHD following oral administration of 300 mg OXZ tablets in healthy adults.[8]

Levetiracetam model

Initial estimates of LogP, $f_{u,p}$, $P_{eff,trans}$, solubility, and dissolution data (as percentage dissolved vs. time) were obtained from the literature. To account for reabsorption, renal CL (CL_R) was parameterized as $CL_R = f_{GFR} \times f_{u,p} \times$ glomerular filtration rate (GFR), where ($1\text{-}f_{GFR}$) represents the fraction of GFR re-absorbed. The initial estimate of f_{GFR} was calculated as the ratio of reported CL_R (of a standard healthy individual) to GFR,[11] as shown in section S1.2 of the ESM. To account for the esterase-mediated metabolism in RBCs, data from a reported whole blood assay that estimated the in vitro metabolic capacity (V_{max}) and affinity (K_m) were used as initial estimates.[9] However, the information about the specific enzyme and its abundance was not available in the literature. Therefore, a generic enzyme was created in PK-Sim's virtual individual, which was assumed to be exclusively localized within the RBCs at a concentration of 1 μmol/L. The final model was developed by optimizing only the V_{max} estimate (while fixing others at the literature value) to simultaneously fit the mean C–T and E–T data from two reported studies that administered a single 2000 mg i.v. infusion and a single 1000 mg tablet of LEV, respectively.[11,13]

External evaluation of the PBPK models

Population simulations were performed in PK-Sim to evaluate the predictive performance of the final models by comparing them with observed data from other reported studies (that were not used for model development) in adults following single[7,9–13,18,19] and multiple doses[12,20] at different dose levels. Virtual cohorts were generated for each study by sampling 100 individuals (50% women) from the PK-Sim population library. Boundaries of available patient characteristics (e.g., age and body weight) of the respective study were applied while sampling the virtual cohorts to resemble the study population. An evaluation was performed by visual inspection (i.e., by comparing the simulated C-T and E-T data with the observed data and the simulated area under the C-T curve [AUC] with the observed AUC).

PBPK model scaling to children

The adult PBPK models for LEV and OXZ were scaled to children and adolescents by accounting for the age-related scaling in the physiological properties, such as organ size and perfusion. Of note, the drug-specific properties remained unchanged as in adults. The scaling of physiology was accounted for when virtual pediatric cohorts were sampled ($n = 100$) from PK-Sim's population library (similar to adult sampling). Notably, no age-related maturation in the drug-metabolizing enzymes was considered in the scaling process. This was not critical because the PBPK models were scaled to 2 years of age and above. Moreover, the bodyweight normalized CL (ml/min/kg) has been reported to be higher in younger children than their older counterparts and adults.[21-23]

Simulations were performed using the PBPK models for children (in the absence of an EIAED effect) and compared with the C-T and E-T data of LEV and MHD obtained from several reported studies that included children of 2 years and above.[21-25] Because OXZ and LEV are mainly used as adjunctive therapy in children, most reported studies included children on concomitant EIAEDs, potentially leading to overprediction of concentrations. Therefore, the potential effect of EIAEDs was estimated by empirically increasing the metabolic clearance parameters V_{max} and $CL_{int,H}$ (for LEV and MHD, respectively), and performing additional simulations to fit the PK profiles. Thus, the percentage increase in systemic CL of LEV and MHD, corresponding to the increase in intrinsic clearance, would represent the estimated effect size of EIAEDs in children.

Simulations of steady-state exposure in children

Steady-state trough concentrations (C_{trough}) of MHD and LEV were simulated using the final models of OXZ and MHD, respectively, with and without considering co-administration of EIAEDs. Simulations were performed using the US Food and Drug Administration's (FDA) maximum recommended doses (MRDs) in children from 2 years of age and above, as summarized in Table S3. For the simulation of each dose group, 1000 virtual children were sampled from PK-Sim's White American population library based on the respective age and bodyweight bands advised by the FDA. The simulated C_{trough} range for each group was compared with the reference range of MHD (3–30 mg/L) and LEV (12–46 mg/L).[26] If any of the recommended doses resulted in C_{trough} range inconsistent with the reference range, then additional doses (not included in the FDA recommendation) were also explored.

RESULTS

Model development and external evaluation

The initial and final estimates of the drug-related properties of OXZ, MHD, and LEV are shown in Tables 1 and

TABLE 1 Initial and final estimates of the drug-related properties characterizing the absorption, distribution, metabolism, and excretion (ADME) of oxcarbazepine (OXZ) and its monohydroxy derivative (MHD) metabolite

Process	Property	Unit	Compound	Initial Estimate	Final Estimate
Distribution, Metabolism and Excretion	LogP	-	OXZ	1.31[8]	1.31
			MHD	0.94[8]	**1.20**
	$f_{u,p}$	-	OXZ	0.35[39]	0.35
			MHD	0.60[40]	0.60
	$CL_{int,AKR1C1}$	µl/min/pmol enzyme	OXZ	9.30[17]	**0.465**
	$CL_{int,AKR1C2}$			10.60[17]	**0.53**
	$CL_{int,AKR1C3}$			7.82[17]	**0.392**
	$CL_{int,AKR1C4}$			2.60[17]	**0.13**
	$CL_{int,H}$	min^{-1}	MHD	0.038[8]	**0.035**[a]
					0.0489[b]
	$CL_{int,R}$			0.058[8]	**0.075**
Absorption	Solubility	mg/ml	OXZ	0.30[15]	0.30
	$T_{50\%}$	min		30[16]	**108**
	Dissolution shape	-		0.80[16]	0.80
	$P_{eff.trans}$	cm. min^{-1}		[c]5.07×10^{-6}	**4.45×10^{-5}**
			MHD	[c]3.79×10^{-6}	[c]3.79×10^{-6}

Note: The initial estimates were derived from the references cited as superscripts. The final estimates in bold letters represent optimized values.

Abbreviations: $CL_{int,AKR1C1}$ to $CL_{int,AKR1C4}$, intrinsic clearance measured with recombinant aldo-keto reductase (family 1) isoforms C1 to C4, respectively; $CL_{int,H}$, intrinsic clearance per unit liver volume; $CL_{int,R}$, intrinsic clearance per unit kidney volume; $f_{u,p}$, free fraction in plasma; LogP, lipid-water partition coefficient; $P_{eff,trans}$, effective (transcellular) intestinal permeability; $T_{50\%}$, time to dissolve 50% of tablet strength.

[a]In the absence of enzyme inducers.

[b]In the presence of enzyme inducers.

[c]PK-Sim generated value.

2. Figures 1 and 2 represent the overlay of the simulated plasma C-T and urinary E-T profiles with the observed clinical data of adults following single doses of MHD, OXZ, and LEV (multiple dosing plots are shown in Figure S2). Overall, the mean predictions and the population variability, as represented by the 90% prediction intervals, were reasonably well-predicted upon visual inspection. Additionally, the predicted mean AUC values were also within a 0.75 to a 1.25-fold range of the observed mean AUC values of the respective studies (Figure S3).

PBPK model scaling to children

The results of the PBPK model scaling to children and adolescents are depicted in Figure 3 and Figure 4 for OXZ and LEV, respectively. In Figure 4a,b, the scaled PBPK model for LEV (in the absence of an EIAED effect) performed reasonably well in predicting the observed data in children 2–6 years and adolescents of 12–16 years of age, who did not receive any concomitant EIAEDs. This ensured that the overall PBPK modeling framework, including the age-dependent scaling of physiology, accurately described the age-related PK changes in children and adolescents. Of note, this evaluation could not be performed for MHD because the reported studies of OXZ did not exclude children on EIAEDs.

As expected, the PBPK model simulated PKs in children and adolescents consistently overpredicted the observed LEV and MHD AUC data from the studies, where patients on concomitant EIAEDs were not excluded (dashed lines in Figure 3 and Figure 4c,d,f). Because the AUC is inversely proportional to overall systemic CL, its overprediction implies an underprediction of the observed CL in the presence of EIAEDs. Interestingly, for LEV, AUC overprediction was also accompanied by an overprediction of the extent of urinary excretion ($\%f_{u,dose}$) (dashed line in Figure 4e,g). For example, the overprediction of the steady-state AUC within a dosing interval ($AUC_{ss,0-\tau}$), and the corresponding overprediction of $\%f_{u,dose}$ in Figure 4f,g were 1.27 and 1.21-fold, respectively, in the absence of EIAEDs in the model (Table S4 in the ESM). Note, $AUC_{ss,0-\tau}$ is a more accurate indicator of CL than AUC after single dose (Figure 4d), given that the latter is subject to extrapolation to infinity that may be erroneous. A similar fold overprediction of both $AUC_{ss,0-\tau}$

TABLE 2 Initial and final estimates of the drug-related properties characterizing the absorption, distribution, metabolism, and excretion (ADME) of levetiracetam (LEV)

Process	Property	Unit	Initial Estimate	Final Estimate
Distribution, Metabolism and Excretion	LogP	-	−0.64[36]	−0.64
	$f_{u,p}$	-	0.966[10]	0.966
	V_{max}	pmol/min/ml	287[9]	**8000**[a]
				16000[b]
	K_m	μmol/L	439[9]	439
	f_{GFR}	-	0.40[11]	0.40
Absorption	Solubility	mg/ml	1040[36]	1040
	$T_{50\%}$	min	5[41]	5
	$T_{90\%}$	min	10[41]	10
	$T_{100\%}$	min	15[41]	15
	$P_{eff,trans}$	cm. min^{-1}	[c]1.84×10^{-7} [42]	[c]1.84×10^{-7}

Note: The final estimates in bold letters represent optimized values.

Abbreviations: f_{GFR}, the fraction of glomerular filtrate that escapes tubular reabsorption; $f_{u,p}$, free fraction in plasma; K_m, the concentration required for half-maximal metabolic rate; LogP, lipid-water partition coefficient; $P_{eff,trans}$, effective (transcellular) intestinal permeability; RBC, red blood cell; $T_{50\%}$ to $T_{100\%}$, time to dissolve 50%, 90%, and 100% of tablet strength, respectively; V_{max}, maximum metabolic rate.

[a]In the absence of enzyme inducers.

[b]In the presence of enzyme inducers.

[c]In situ rat intestinal perfusion assay result.

and $\%f_{u,dose}$ implies that CL_R was well-predicted, because $CL_R = dose \times f_{u,dose} / AUC_{ss,0-\tau}$. This further confirmed that the overprediction of AUC (i.e., reflective of underprediction of overall CL) by the model was linked to underprediction of metabolic CL (CL_M), because $CL = CL_M + CL_R$, and given that CL_R was unchanged. Therefore, further empirical adjustments were made to the V_{max} (representing LEV metabolism in RBCs) and $CL_{int,H}$ (representing MHD metabolism in the liver) estimates that were optimized previously in adults (Tables 1 and 2). A 2-fold and 1.4-fold increase in the V_{max} and $CL_{int,H}$ estimates, respectively, could resolve the overprediction of AUC and $\%f_{u,dose}$ to a reasonable extent (the solid red lines in Figures 3 and 4c through 4g). These empirical adjustments led to an average increase in the overall CL (i.e., the effect size of the EIAEDs), estimated to be about 25% for MHD and 20%–30% for LEV (Figure S4). However, the individual estimates of the effect size had a wide range, ranging from 16%–34% for MHD and 10%–80% for LEV, suggesting a clinically relevant drug-drug interaction (DDI).

Unlike for AUC and $\%f_{u,dose}$, no clear trend of over- or underprediction was observed for the peak concentrations (C_{max}). However, that did not impact the overall goal of the analysis, which was to understand the change in CL due to EIAEDs, because the maintenance doses of the AEDs are adjusted for a change in CL in pediatric patients. Theoretically, C_{max} is not a reliable indicator of CL change because of its significant dependence on absorption rate and volume of distribution. Therefore, the current conclusions were entirely made based on the change in AUC and $\%f_{u,dose}$, which are impacted by CL for fully bioavailable drugs like MHD and LEV.

Simulations of steady-state exposure in children

The simulated exposures for the MRDs and additional doses are shown in Figure 5. As expected, the simulated C_{trough} values of MHD and LEV were higher when the effect of EIAEDs was not considered in the model. The simulated concentrations of MHD were still within the reference range in children above 4 years of age at the MRDs. However, MHD concentrations crossed the reference limit in about 12% of virtual children between 2 and 4 years of age, at the MRD of 60 mg/kg/day in the absence of EIAEDs. Additional simulations revealed that the number of virtual children exceeding the reference limit would be marginal (~3%) at an alternative maximum dose of 45 mg/kg/day.

On the other hand, LEV concentrations in the same age group (i.e., 2–4 years), who are on concomitant EIAEDs, remained on the lower side of the reference range at the MRD of 50 mg/kg/day. However, when children above 4 years of age are not receiving any concomitant EIAED, the MRD of 60 mg/kg/day resulted in higher exposure than required in about 25% of children. Exploratory

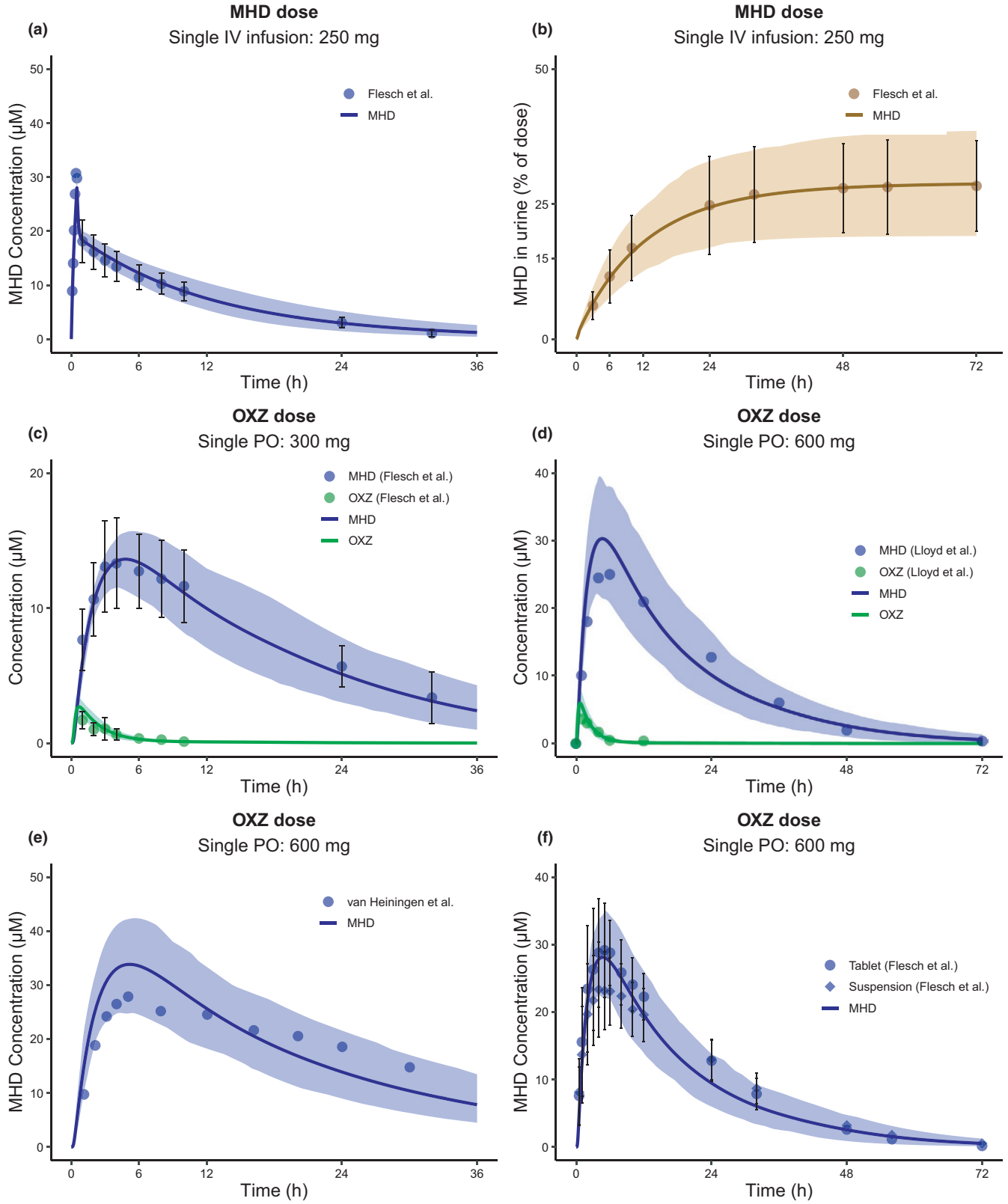

FIGURE 1 Visual inspection of the final model predictions for oxcarbazepine (OXZ) and its monohydroxy derivative (MHD) metabolite using observed data (solid circles) from several clinical studies in adults following a single dose. The arithmetic mean (solid lines) and the 90% prediction interval (shaded areas) following intravenous (i.v.) administration of MHD (a, b) and oral (p.o.) administration of OXZ (c, d, e, f) are shown. The error bars represent the reported standard deviation in the clinical studies (if available). Data Sources: Flesch et al.,[8,38] Lloyd et al.,[12] and van Heiningen et al.[18]

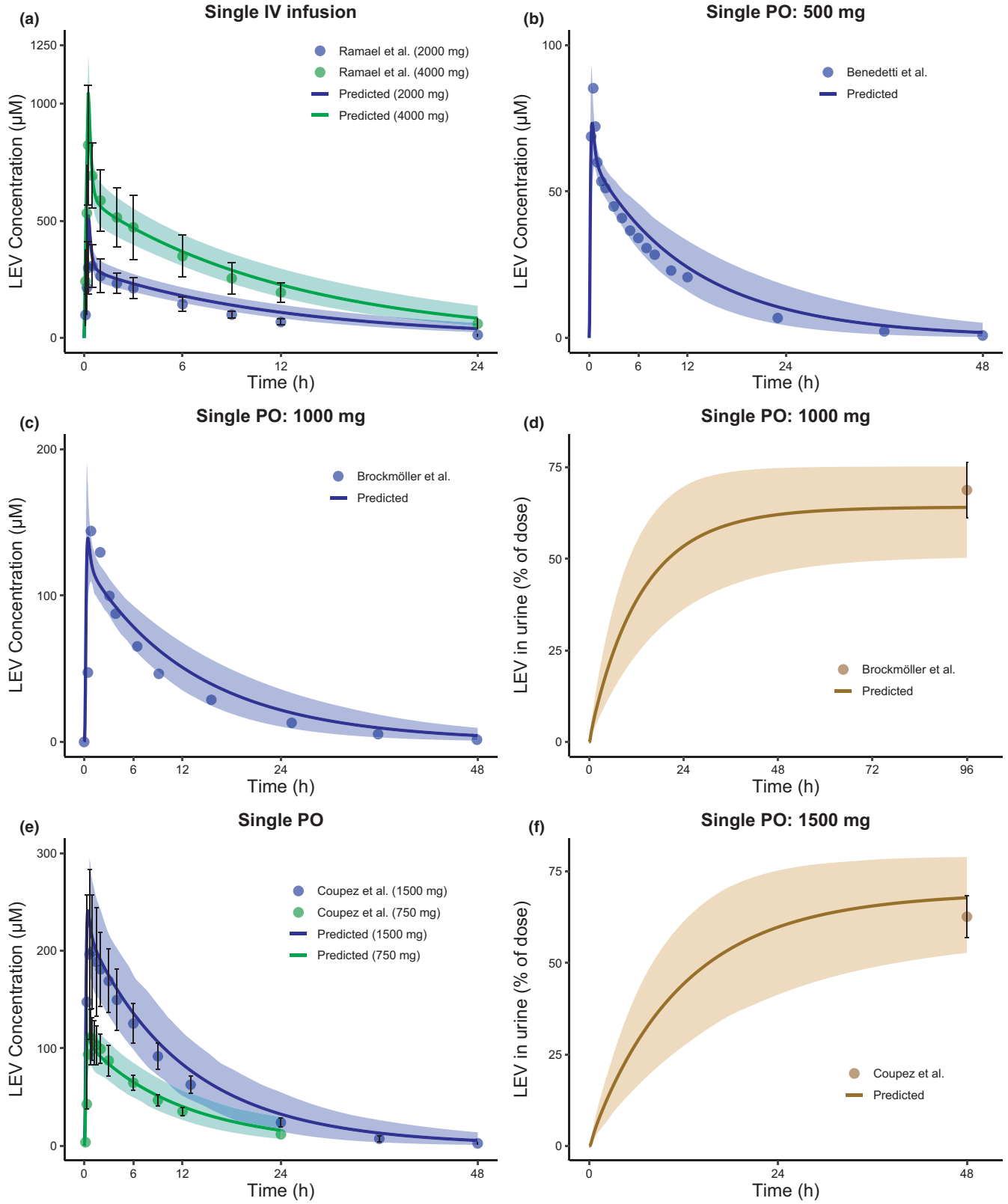

FIGURE 2 Visual inspection of the final model predictions for levetiracetam (LEV) using observed data (solid circles) from several clinical studies in adults following a single dose. The arithmetic mean (solid lines) and the 90% prediction interval (shaded areas) of the predicted plasma concentrations (a, b, c, e) and urinary excretion (d, f) following intravenous (i.v.) (a) and oral (p.o.) administration (b, c, d, e, f) of LEV are shown. The error bars represent the reported standard deviation in the clinical studies (if available). Data Sources: Ramael et al.,[13] Benedetti et al.,[10] Brockmöller et al.,[11] and Coupez et al.[9,19]

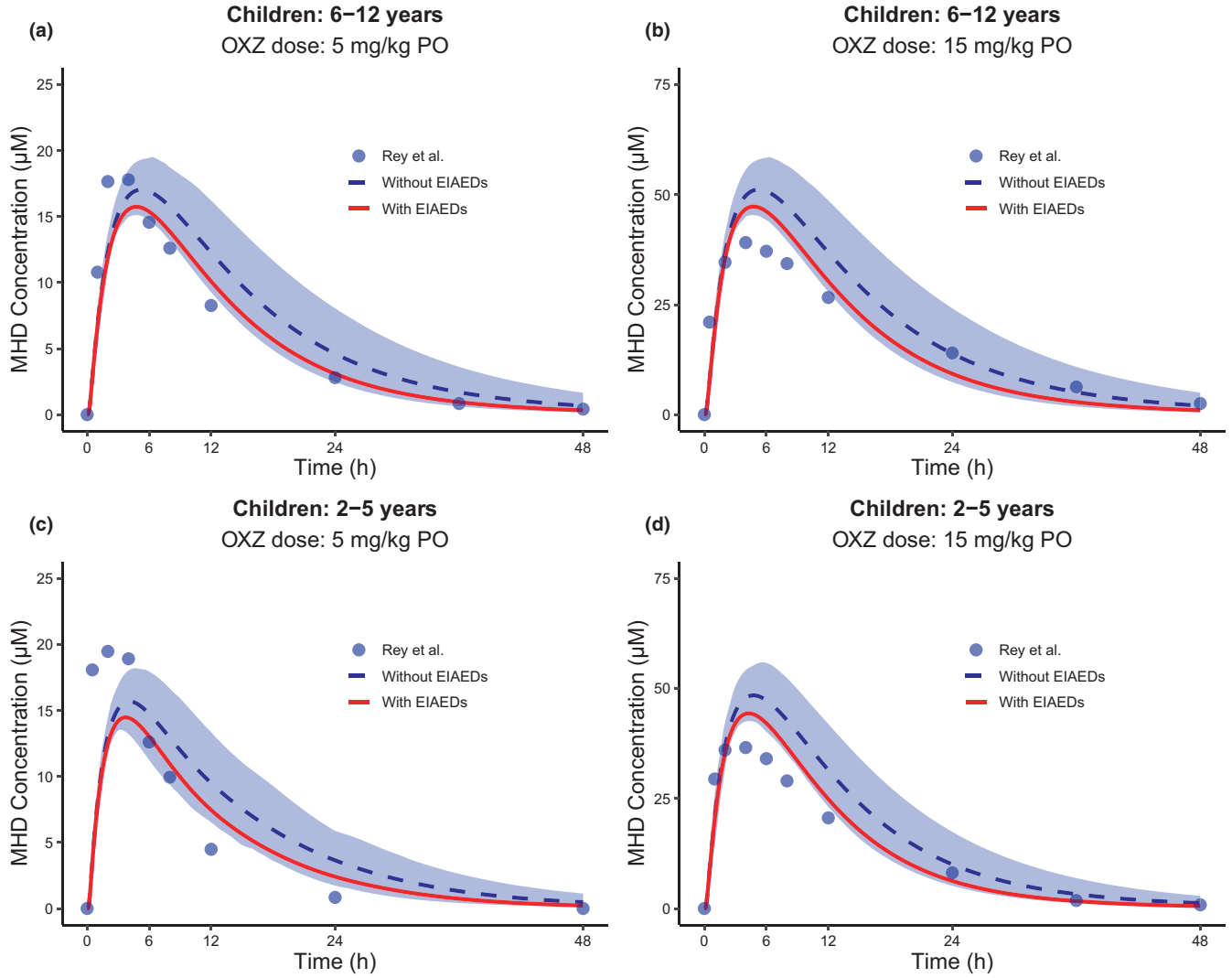

FIGURE 3 Prediction of plasma concentration-time profiles of the monohydroxy derivative (MHD) metabolite of oxcarbazepine (OXZ) in children of 2–5 years (c, d) and 6–12 years (a, b) of age following a single oral (p.o.) administration of OXZ at 5 and 15 mg/kg doses. The dashed line represents the mean prediction when only age-dependent extrapolation of the pharmacokinetics (PKs) was considered along with the 90% prediction interval (shaded area). The solid red line represents the mean prediction when the additional effect of enzyme-inducing anti-epileptic drugs (EIAEDs) was considered. Solid circles represent the observed clinical data reported by Rey et al.[24] Standard deviation was not reported in the original data

simulations revealed that a bodyweight-based dose band would help achieve LEV concentrations within the range. The number of virtual children at risk of exceeding the reference range would be minimal (~5%). The maximum doses would be 50 mg/kg/day and 1250 mg/day for children below and above 50 kg, respectively, above 4 years of age.

DISCUSSION

To our knowledge, this is the first application of PBPK modeling to elucidate the influence of age and co-administration of EIAEDs on the PKs of two new-generation AEDs (OXZ and LEV) in children (2 years of age and above) and adolescents. The PBPK modeling results suggest that age alone influences the weight-normalized CL of MHD and LEV in the absence of any concomitant EIAEDs (Figure S4). Younger children have a higher baseline CL (ml/min/kg) than their older counterparts and adults, and concomitant EIAEDs further increase CL by 25% for MHD and 20%–30% for LEV at any age. Therefore, children who are not on the adjunctive therapy with an EIAED are likely to maintain a higher exposure of MHD and LEV at steady-state conditions (Figure 5). This would have potential implications during dose escalation.

Therapeutic drug monitoring for either of these drugs is not routinely performed. This is because the "therapeutic range" of concentrations is not well-defined for these

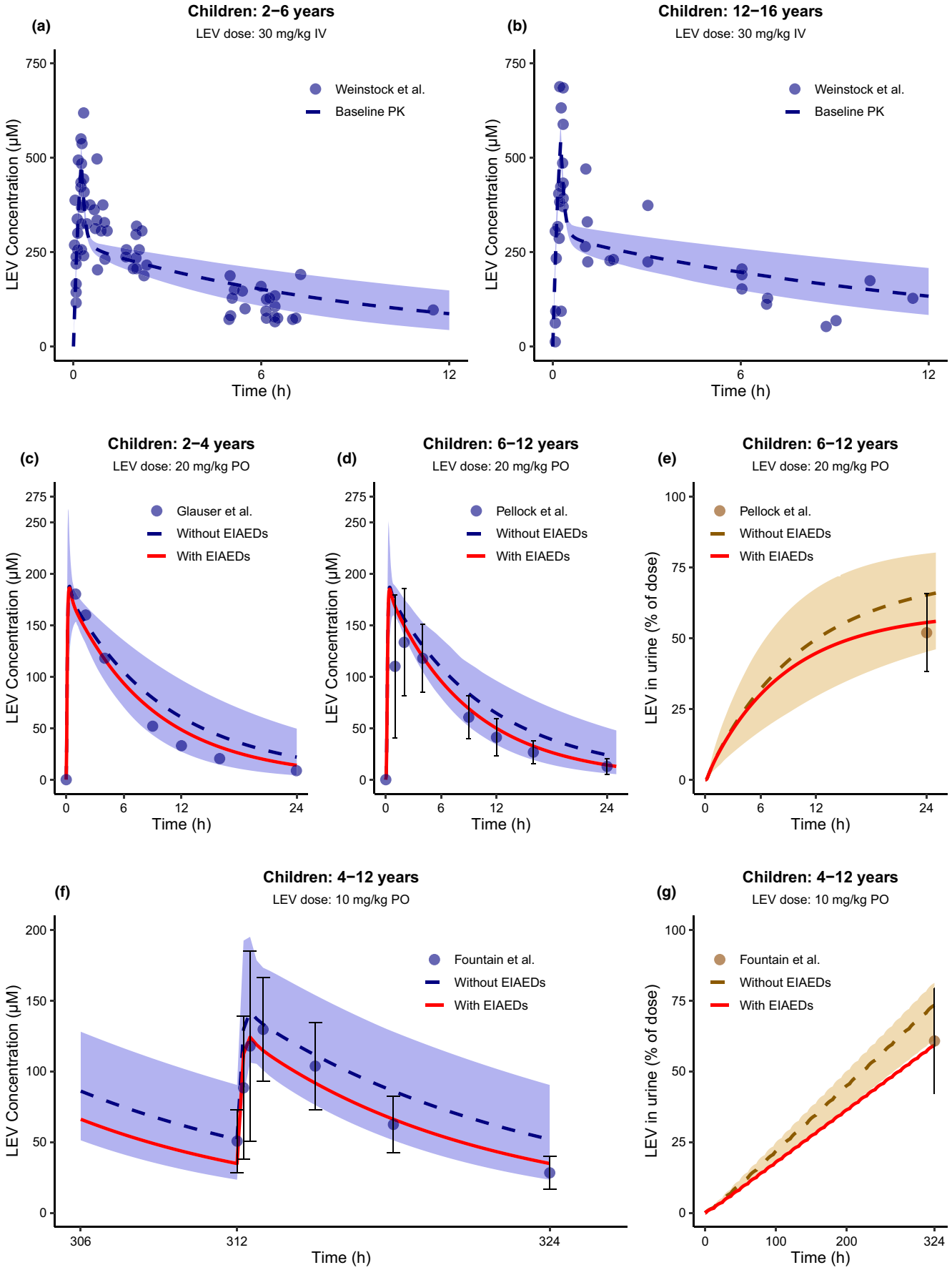
(a)
Children: 2−6 years
LEV dose: 30 mg/kg IV
Weinstock et al.
Baseline PK
LEV Concentration (μM)
Time (h)
(b)
Children: 12−16 years
LEV dose: 30 mg/kg IV
Weinstock et al.
Baseline PK
LEV Concentration (μM)
Time (h)
(c)
Children: 2−4 years
LEV dose: 20 mg/kg PO
Glauser et al.
Without EIAEDs
With EIAEDs
LEV Concentration (μM)
Time (h)
(d)
Children: 6−12 years
LEV dose: 20 mg/kg PO
Pellock et al.
Without EIAEDs
With EIAEDs
LEV Concentration (μM)
Time (h)
(e)
Children: 6−12 years
LEV dose: 20 mg/kg PO
Pellock et al.
Without EIAEDs
With EIAEDs
LEV in urine (% of dose)
Time (h)
(f)
Children: 4−12 years
LEV dose: 10 mg/kg PO
Fountain et al.
Without EIAEDs
With EIAEDs
LEV Concentration (μM)
Time (h)
(g)
Children: 4−12 years
LEV dose: 10 mg/kg PO
Fountain et al.
Without EIAEDs
With EIAEDs
LEV in urine (% of dose)
Time (h)

FIGURE 4 Prediction of plasma concentration time (a, b, c, d, f) and urinary excretion time (e, g) profiles in children ranged between 2 and 16 years of age following a single intravenous (i.v.) infusion (a, b), a single oral (c, d, e), and multiple oral (f, g) administrations of levetiracetam (LEV). The dashed line represents the mean prediction when only age-dependent extrapolation of the pharmacokinetics (PKs) was considered, and the shaded area is the 90% prediction interval. The red line represents the mean prediction when the additional effect of enzyme-inducing anti-epileptic drugs (EIAEDs) was considered. The solid circles represent the observed clinical data. The study by Weinstock et al.[25] (a, b) excluded children on concomitant EIAEDs, whereas studies by Glauser et al.,[21] Fountain et al.,[23] and Pellock et al.[22] did not exclude such patients

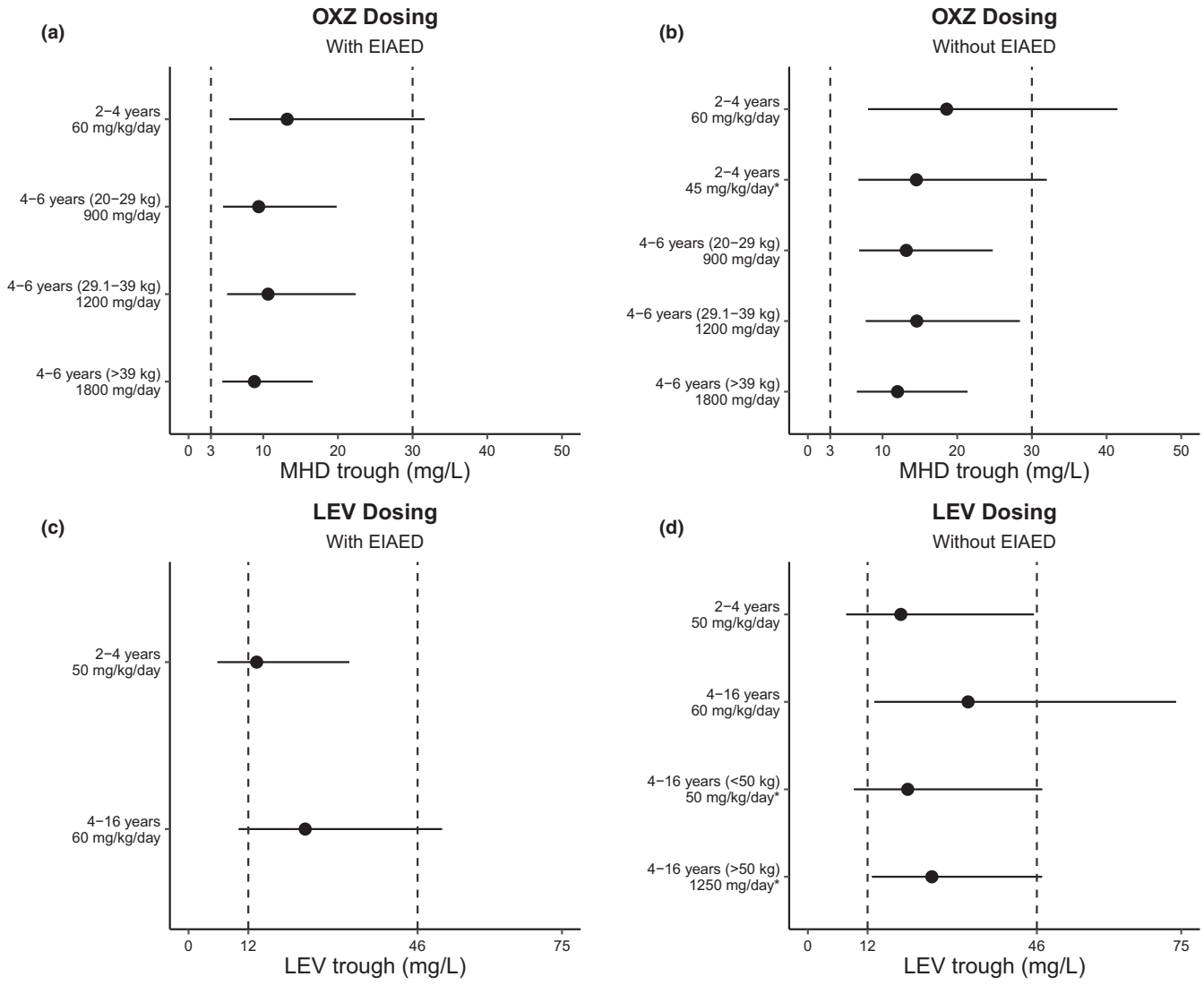

FIGURE 5 Simulated trough concentrations of monohydroxy derivative (MHD) and levetiracetam (LEV) at steady-state following oral administration of oxcarbazepine (OXZ) and LEV, with and without co-administration of enzyme-inducing anti-epileptic drugs (EIAEDs). The solid circle and the solid line represent the median predicted concentration and the 95% prediction interval, respectively. The dashed lines define the reference range of concentrations of MHD and LEV as per recommendations of the International League Against Epilepsy[26] and Striano et al.[30] Dosing schemes include both the US Food and Drug Administration's (FDA) maximum recommended doses (MRDs) and additional exploratory doses (marked with an asterisk), which were tested when a maximum recommended dose tends to exceed the reference range. All doses were administered in two divided doses separated at 12 h intervals as per the FDA recommendation

AEDs, as the range largely varied between individuals in previous clinical trials.[14,26–29] Therefore, in practice, doses are gradually titrated upward based on response (e.g., optimal seizure control) and then maintained at a stable dose. Therefore, it is important to assess the safe range of doses in children. The International League Against Epilepsy (ILAE) proposed a broad "reference range" for steady-state concentrations of these AEDs informed by the

individual "therapeutic range" for most patients studied in previous clinical trials. The proposed ranges are 3–35 and 12–46 mg/L for MHD and LEV, respectively,[26] which were initially considered in this work for assessing the MRDs shown in Table S3. For OXZ, it was further defined that the adverse effects typically start at an MHD concentration of 30 mg/L.[30] Therefore, a more conservative "reference range" (i.e., 3–30 mg/L) for OXZ was considered in this work. Simulation results indicate that children between 2 and 4 years and above 4 years of age, who are not on concomitant EIAEDs, are at risk of exceeding the reference range for MHD and LEV, respectively, with the current MRD of 60 mg/kg/day. Exploratory simulations suggest that an alternative maximum dose of 45 mg/kg/day for OXZ, 50/mg/kg/day (<50 kg) and 1250 mg/day (>50 kg) for LEV can be considered for these subgroups, respectively. Caution may need to be taken while titrating doses beyond these recommended upper limits, such as monitoring for adverse effects with or without therapeutic drug monitoring. On the other hand, LEV dose escalation could potentially be performed more safely in children between 2 and 4 years who are on EIAEDs, because simulated concentrations at the MRD of 50 mg/kg/day were at the lower side of the reference range.

This work also demonstrates how mechanism-based modeling using a PBPK framework can be utilized in understanding the age-related variation in the effect of a comedication, if any. Theoretically, age would influence the effect of an interacting comedication if the victim drug's fraction of dose eliminated ($f_{e,\text{dose}}$) by the perturbed pathway changes with age.[31] Given the structural and functional changes occurring in the drug-eliminating organs during childhood, an age effect can exist depending on the elimination pathways involved. For example, the average effect size of EIAEDs on LEV's CL (ml/min/kg) was 20% in a 2-year-old child, which increased to 30% in an adolescent (Figure S4). This was expected because the $f_{e,\text{dose}}$ by RBC-mediated metabolism of LEV should increase with age during childhood because of an increase in RBC volume (ml/kg) and a decrease in kidney volume (ml/kg) happening simultaneously up to adolescence as the child grows (Figure S5). On the contrary, the same comedication effect on MHD's CL remains unchanged at 25%. A fixed-effect size (i.e., 25% increase in CL) across the pediatric age is underpinned by the parallel decrease in the liver and kidney volumes (ml/kg) during growth of children, essentially keeping the relative contribution of the liver metabolism (i.e., $f_{e,\text{dose}}$) on overall CL of MHD (ml/min/kg) unaffected by age.

Another advantage is that PBPK modeling can complement the findings of population PK analyses, where the estimates of the comedication effects can be limited by the available pediatric data. For example, the reported estimates of the effect size of EIAEDs on MHD's CL varied two-fold from 17% to 35% across various population PK analyses in children.[32-34] The available data might have caused such inter-study variation in the estimate. The likely effect size has been elucidated to be 25% by the current PBPK modeling. In addition, for LEV's CL, the present finding aligns with a previous population PK analysis, which estimated a gross 22% increase in CL with concomitant use of EIAEDs in children.[35]

Overall, the initial estimates of the model parameters remained unaltered except for the CL-related parameters of MHD ($CL_{int,H}$ and $CL_{int,R}$), OXZ ($CL_{int,AKR}$), and LEV (V_{max}), and the absorption-related parameters of OXZ that had to be optimized (Tables 1 and 2). For MHD, the initial estimates of $CL_{int,H}$ and $CL_{int,R}$ were back-calculated from in vivo CL data assuming the physiology of a standard 73 kg adult implemented in PK-Sim's default settings, which might have caused the difference while fitting the real-world clinical trial data. For OXZ, the initial estimates of $CL_{int,AKR}$ (μl/min/pmol AKR) were optimized while keeping the enzyme abundance [AKR] fixed to an arbitrary value of 1 μmol/L tissue (i.e., PK-Sim's default setting in the absence of abundance information). Because both $CL_{int,AKR}$ and [AKR] are variables in the calculation of organ-level intrinsic clearance ($CL_{int,org}$ in Equation 2 in the ESM), and the AKR was fixed during optimization, a 20-fold lower optimized value of $CL_{int,AKR}$ (Table 1) most likely reflects a lower AKR of the AKR1C isoforms in vivo than the default value used. It can also reflect a disconnect between the respective enzyme's functional form (i.e., post-translationally modified protein) than the genetic form (e.g., mRNA) imported from the Open Systems Pharmacology gene expression database. Similarly, for the relationship that dictates the scaling of LEV's clearance (Equations 5 and 6 in ESM), a 28-fold higher V_{max} estimate most likely reflects a wider presence of type B esterase-mediated metabolism beyond that occurring in RBCs. LEV metabolism was assumed to occur exclusively in RBCs because its metabolic turnover was observed only in a whole blood incubation (and not in plasma and liver homogenate).[9] However, that does not rule out the involvement of other tissues in LEV's metabolism, which is a potential area for future evaluation.[10] OXZ is a poorly soluble compound (0.30 mg/ml),[15] and its immediate-release tablet and suspension formulations are not bioequivalent in terms of rate of absorption (i.e., peak concentration). However, they are equivalent based on the extent of absorption (i.e., AUC).[7] This implies a possible in vitro-in vivo disconnect in the dissolution profile of OXZ, which might have caused a poor fit when in vitro dissolution data were directly used. Thus, a Weibull model was used in the final model, where the in vitro $T_{50\%}$ (30 min) was optimized to 108 min to account for the

possible slow dissolution process in vivo. This issue was not evident for LEV, based on its high solubility (1040 mg/ml)[36] and established bioequivalence between formulations,[19] which led to the use of in vitro dissolution data in the final model without any optimization. The permeability ($P_{eff,trans}$) estimate was available for LEV from an in situ rat intestinal perfusion study (1.84×10^{-7} cm/min). However, it was not available for OXZ and MHD, which led to the use of PK-Sim generated $P_{eff,trans}$ estimates initially (5.07×10^{-6} and 3.79×10^{-6}, respectively); however, OXZ's permeability had to be optimized to one log-fold higher value (4.45×10^{-5} cm/min) to improve the fit. A one log-fold higher value of $P_{eff,trans}$ for OXZ compared to MHD is anticipated because the former is more lipophilic than the latter.

It is noteworthy that the effect of enzyme induction was included in the model as a gross effect of EIAEDs, irrespective of the specific inducer (e.g., carbamazepine or phenytoin or phenobarbital), and also regardless of the number of EIAEDs used at the same time (i.e., absence of additive inductive effect). Such an approximation is well supported by a previous study by Perucca et al.,[37] where the effect of various EIAEDs was assessed (both separately and collectively) on antipyrine CL, a model compound used to evaluate hepatic oxidative metabolism. In that study, the extent of increase in antipyrine CL was not meaningfully different when various EIAEDs were administered separately and when they were co-administered together. Of note, previous population PK analyses also assumed a universal covariate effect for the enzyme inducers.[32-35]

A limitation of this work was that the applicability of the models is limited to children of 2 years of age and above. The UGT isoforms responsible for MHD's metabolism have not been identified,[8] resulting in a lack of understanding of the maturation of MHD's metabolism in neonates and infants. In addition, the maturation of the RBC-esterases and tubular reabsorption (for LEV) has not been well-characterized. Moreover, the exact mechanisms of LEV's high extent of re-absorption ($f_{GFR} = 0.4$) is also unclear, given the hydrophilic nature (Log$P = -0.64$) of this compound. Therefore, it is important to know if any active process is involved, which might have additional implications for maturation. Future research can facilitate the extension of these models to neonates and infants. Another limitation was that the effect size of EIAEDs on CL of MHD and LEV were empirically estimated by comparing the model predictions in the absence of an EIAED effect with the reported mean C-T data from the respective pediatric studies, where 100% of the participants were not taking concomitant EIAEDs. Therefore, the current effect size of 25% and 20%–30% increase in CL of MHD and LEV, respectively, could have been underestimated.

CONCLUSION

PBPK modeling was successfully used to predict the age-related changes in the PKs of LEV, OXZ, and its active metabolite MHD in children of 2 years of age and above by leveraging data from the literature. The results indicate that younger children have higher weight-normalized CL (ml/min/kg) than their older counterparts and adults, and concomitant use of EIAEDs further increase the CL of both MHD and LEV. Therefore, in general, dose escalation should be performed cautiously in children who are not receiving concomitant EIAEDs to minimize the risk of exceeding the reference range of steady-state concentrations at the MRD. On the other hand, dose-escalation may be safer in children who are on concomitant EIAEDs.

Interestingly, PBPK modeling revealed that the increase in LEV's CL due to concomitant use of EIAEDs is dependent on age, which steadily rises from 20% (at 2 years) to a stable effect size of 30% at adolescence. The age-dependent effect of comedications is pertinent to the biological processes involved in LEV's elimination (i.e., changing RBC volume with age). On the other hand, the effect of EIAEDs on MHD's CL remains fixed at 25% at any age. These findings further confirm that DDIs may or may not depend on age in children depending on the drug's disposition. Therefore, a systematic approach to assessing the age-dependent DDI potential for other drugs can help to optimize drug dosing, including through the application of PBPK modeling.

ACKNOWLEDGEMENTS

None to declare.

CONFLICT OF INTEREST

The authors declared no competing interests for this work.

AUTHOR CONTRIBUTIONS

J.S. and D.G. wrote the manuscript. J.S. and D.G. designed the research. J.S., E.K., and D.G. performed the research. J.S. and E.K. analyzed the data.

ETHICAL APPROVAL

No new subject enrollment took place as part of this study. The institutional review board approved the PBPK modeling research at the University of North Carolina at Chapel Hill.

CONSENT TO PARTICIPATE

No new subject enrollment took place as part of this study.

REFERENCES

1. U.S. Food and Drug Administration TRILEPTAL® prescribing information. In: Drugs@FDA. https://www.accessdata.fda.gov/drugsatfda_docs/label/2017/021014s036lbl.pdf. Accessed August 8, 2021.
2. U.S. Food and Drug Administration. KEPPRA® prescribing information. In: Drugs@FDA. https://www.accessdata.fda.gov/drugsatfda_docs/label/2017/021035s099021505s038lbl.pdf. Accessed August 8, 2021.
3. Krämer G. The limitations of antiepileptic drug monotherapy. *Epilepsia*. 1997;38:S9-S13.
4. Schütz H, Feldmann K, Faigle J, Kriemler H-P, Winkler T. The metabolism of ^{14}C-oxcarbazepine in man. *Xenobiotica*. 1986;16(8):769-778.
5. Faigle JW, Menge GP. Metabolic characteristics of oxcarbazepine (TRILEPTAL®) and their beneficial implications for enzyme induction and drug interactions. *Behav Neurol*. 1990;3(1):21-30.
6. Barski OA, Tipparaju SM, Bhatnagar A. The aldo-keto reductase superfamily and its role in drug metabolism and detoxification. *Drug Metab Rev*. 2008;40(4):553-624.
7. Flesch G. Overview of the clinical pharmacokinetics of oxcarbazepine. *Clin Drug Investig*. 2004;24(4):185-203.
8. Flesch G, Czendlik C, Renard D, Lloyd P. Pharmacokinetics of the monohydroxy derivative of oxcarbazepine and its enantiomers after a single intravenous dose given as racemate compared with a single oral dose of oxcarbazepine. *Drug Metab Dispos*. 2011;39(6):1103-1110.
9. Coupez R, Nicolas JM, Browne TR. Levetiracetam, a new antiepileptic agent: Lack of in vitro and in vivo pharmacokinetic interaction with valproic acid. *Epilepsia*. 2003;44(2):171-178.
10. Benedetti MS, Whomsley R, Nicolas J-M, Young C, Baltes E. Pharmacokinetics and metabolism of ^{14}C-levetiracetam, a new antiepileptic agent, in healthy volunteers. *Eur J Clin Pharmacol*. 2003;59(8):621-630.
11. Brockmoller J, Thomsen T, Wittstock M, Coupez R, Lochs H, Roots I. Pharmacokinetics of levetiracetam in patients with moderate to severe liver cirrhosis (Child-Pugh classes A, B, and C): characterization by dynamic liver function tests. *Clin Pharmacol Ther*. 2005;77(6):529-541.
12. Lloyd P, Flesch G, Dieterle W. Clinical pharmacology and pharmacokinetics of oxcarbazepine. *Epilepsia*. 1994;35:S10-S13.
13. Ramael S, Daoust A, Otoul C, et al. Levetiracetam intravenous infusion: a randomized, placebo-controlled safety and pharmacokinetic study. *Epilepsia*. 2006;47(7):1128-1135.
14. Patsalos PN. Clinical pharmacokinetics of levetiracetam. *Clin Pharmacokinet*. 2004;43(11):707-724.
15. Mohan A, Sangeetha G. In vitro-in vivo evaluation of fast-dissolving tablets containing solid dispersion of oxcarbazepine. *Int J Pharm Pharm Sci*. 2016;8:124-131.
16. Patel N, Chotai N, Patel J, et al. Comparison of in vitro dissolution profiles of oxcarbazepine HP-beta-CD tablet formulations with marketed oxcarbazepine tablets. *Dissol Technol*. 2008;15:28-34.
17. Malátková P, Havlíková L, Wsól V. The role of carbonyl reducing enzymes in oxcarbazepine in vitro metabolism in man. *Chem Biol Interact*. 2014;220:241-247.
18. van Heiningen PN, Eve MD, Oosterhuis B, et al. The influence of age on the pharmacokinetics of the antiepileptic agent oxcarbazepine. *Clin Pharmacol Ther*. 1991;50(4):410-419.
19. Coupez R, Straetemans R, Sehgal G, Stockis A, Lu ZS. Levetiracetam: relative bioavailability and bioequivalence of a 10% oral solution (750 mg) and 750-mg tablets. *J Clin Pharmacol*. 2003;43(12):1370-1376.
20. Rouits E, Burton I, Guénolé E, et al. Pharmacokinetics of levetiracetam XR 500 mg tablets. *Epilepsy Res*. 2009;84(2–3):224-231.
21. Glauser TA, Mitchell WG, Weinstock A, et al. Pharmacokinetics of levetiracetam in infants and young children with epilepsy. *Epilepsia*. 2007;48(6):1117-1122.
22. Pellock JM, Glauser TA, Bebin EM, et al. Pharmacokinetic study of levetiracetam in children. *Epilepsia*. 2001;42(12):1574-1579.
23. Fountain NB, Conry JA, Rodríguez-Leyva I, et al. Prospective assessment of levetiracetam pharmacokinetics during dose escalation in 4-to 12-year-old children with partial-onset seizures on concomitant carbamazepine or valproate. *Epilepsy Res*. 2007;74(1):60-69.
24. Rey E, Bulteau C, Motte J, et al. Oxcarbazepine pharmacokinetics and tolerability in children with inadequately controlled epilepsy. *J Clin Pharmacol*. 2004;44(11):1290-1300.
25. Weinstock A, Ruiz M, Gerard D, et al. Prospective open-label, single-arm, multicenter, safety, tolerability, and pharmacokinetic studies of intravenous levetiracetam in children with epilepsy. *J Child Neurol*. 2013;28(11):1423-1429.
26. Patsalos PN, Berry DJ, Bourgeois BF, et al. Antiepileptic drugs—best practice guidelines for therapeutic drug monitoring: A position paper by the Subcommission on Therapeutic Drug Monitoring, ILAE commission on therapeutic strategies. *Epilepsia*. 2008;49(7):1239-1276.
27. May TW, Korn-Merker E, Rambeck B. Clinical pharmacokinetics of oxcarbazepine. *Clin Pharmacokinet*. 2003;42(12):1023-1042.
28. Bring P, Ensom MH. Does oxcarbazepine warrant therapeutic drug monitoring? *Clin Pharmacokinet*. 2008;47(12):767-778.
29. Perrenoud M, André P, Buclin T, et al. Levetiracetam circulating concentrations and response in status epilepticus. *Epilepsy Behav*. 2018;88:61-65.
30. Striano S, Striano P, Di Nocera P, et al. Relationship between serum mono-hydroxy-carbazepine concentrations and adverse effects in patients with epilepsy on high-dose oxcarbazepine therapy. *Epilepsy Res*. 2006;69(2):170-176.
31. Gonzalez D, Sinha J. Pediatric drug-drug interaction evaluation: drug, patient population, and methodological considerations. *J Clin Pharmacol*. 2021;61(S1):S175-S187.
32. Wang Y, Zhang H-N, Niu C-H, et al. Population pharmacokinetics modeling of oxcarbazepine to characterize drug interactions in Chinese children with epilepsy. *Acta Pharmacol Sin*. 2014;35(10):1342-1350.
33. Sugiyama I, Bouillon T, Yamaguchi M, et al. Population pharmacokinetic analysis for 10-monohydroxy derivative of oxcarbazepine in pediatric epileptic patients shows no difference between Japanese and other ethnicities. *Drug Metab Pharmacokinet*. 2015;30(2):160-167.
34. Park K-J, Kim J-R, Joo EY, et al. Drug interaction and pharmacokinetic modeling of oxcarbazepine in Korean patients with epilepsy. *Clin Neuropharmacol*. 2012;35(1):40-44.
35. Toublanc N, Sargentini-Maier ML, Lacroix B, Jacqmin P, Stockis A. Retrospective population pharmacokinetic analysis

of levetiracetam in children and adolescents with epilepsy. *Clin Pharmacokinet*. 2008;47(5):333-341.
36. U.S. Food and Drug Administration. Review of environmental assessment for KEPPRA® oral solution (NDA 021-505). In: Drugs@FDA. https://www.accessdata.fda.gov/drugsatfda_docs/nda/2003/021505_s000_keppra_eafonsi.pdf. Accessed May 23, 2021.
37. Perucca E, Hedges A, Makki K, et al. A comparative study of the relative enzyme inducing properties of anticonvulsant drugs in epileptic patients. *Br J Clin Pharmacol*. 1984;18(3):401-410.
38. Flesch G, Tudor D, Denouel J, Bonner J, Camisasca R. Assessment of the bioequivalence of two oxcarbazepine oral suspensions versus a film-coated tablet in healthy subjects. *Int J Clin Pharmacol Ther*. 2003;41(7):299-308.
39. Kalis MM, Huff NA. Oxcarbazepine, an antiepileptic agent. *Clin Ther*. 2001;23(5):680-700.
40. Marvanova M. Pharmacokinetic characteristics of antiepileptic drugs (AEDs). *Ment Health Clin*. 2016;6(1):8-20.
41. Poongothai S, Balaji V, Madhavi B, Reddy AR, Ilavarasan R, Karrunakaran CM. A sensitive dissolution test method for the development and validation of levetiracetam tablets by reverse phase-HPLC technique. *Int J Pharm Tech Res*. 2011;3:1023–1032.
42. Petruševska M, Berglez S, Krisch I, et al. Biowaiver monographs for immediate release solid oral dosage forms: levetiracetam. *J Pharm Sci*. 2015;104(9):2676-2687.

SUPPORTING INFORMATION

Additional supporting information may be found in the online version of the article at the publisher's website.

How to cite this article: Sinha J, Karatza E, Gonzalez D. Physiologically-based pharmacokinetic modeling of oxcarbazepine and levetiracetam during adjunctive antiepileptic therapy in children and adolescents. *CPT Pharmacometrics Syst Pharmacol*. 2022;11:225-239. doi:10.1002/psp4.12750